

Electron Accerelation by V_pxB scheme

N.Yugami and Y.Nishida

Utsunomiya University.

Facility of Engineering, Electrical and Electronic Engineering
2743 Ishii-machi, Utsunomiya, Tochigi, 321, Japan

Abstract

A new type electron linear accelerator, based on v_pxB acceleration mechanism observed originally in plasma, has been demonstrated in vacuum. In this scheme a static magnetic field is applied vertically to the wave propagating direction and the particles are accelerated along the wave front at constant phase with respect to the wave. The linac consists of electron gun, magnetron for a RF source, slow wave structure and a pair of coil for an applied magnetic field. Energy gain of 12.8 keV is observed at an initial energy of 66 keV when an external magnetic field of 2.5 G is applied. The energy gain is 30 % higher than that of a conventional linac. The output energy increment is proportional to the square of the applied magnetic field B₀. Experiments have been carried out with two different RF power levels in order to examine a trapping condition of the v_pxB scheme, which depends on the wave electric field and the applied magnetic field. The comparisons between the experimental and theoretical values are given.

I. Introduction

Recent interests of charged particle accelerators are focused on generating a much higher acceleration gradient. In the last decade some of new acceleration schemes using a longitudinal electric field of the wave, including a plasma wake field accelerator (PWFA), a plasma beat wave accelerator (PBWA) and a v_pxB scheme (or a surfatron), have been proposed.¹⁻⁸⁾ In addition to them, a possibility of the charged particle acceleration using a transverse electric field with a weak external magnetic field has also been proposed.⁹⁾ Some of the experimental results based on the above mentioned scheme have been reported to give the higher acceleration gradient. The new schemes using plasmas can be expected to generate much higher electric field, but it is also easy to predict some difficulties of controlling plasma parameters. The v_pxB acceleration phenomena have been observed in the experiments of microwave-plasma interaction.^{10,11)} In this scheme a static magnetic field is applied vertically to the wave propagating direction and the particles are accelerated along the wave front at constant phase with respect to the wave, and the acceleration continues until the trapping condition breaks. The condition can be determined by the strength of the electric field of the wave, the wave phase velocity and the applied magnetic field. In this mechanism the existence of the plasma is not necessarily essential, therefore the charged particle could be accelerated even in vacuum and the preliminary experimental results have been reported.⁷⁾

Theory of v_pxB Acceleration

In the v_pxB system a charged particle is trapped in an electromagnetic wave (TM wave) with a phase velocity v_p propagating in the z direction immersed in a static magnetic field B₀ in the x direction (Fig. 1). The Lorentz force F_y=qv_zB₀ accelerates the particle in the y direction, and the resulting velocity v_y produces the Lorentz force in the -z direction. If the wave electric field satisfies the following condition, the charged particle is trapped in

the electric field in phase space,

$$E_m > \gamma_p B_0 v_y \quad (1)$$

where E_m, γ_p, v_y are the maximum electric field of the wave, the relativistic factor defined by γ_p = (1-v_p²/c²)^{-0.5} and the velocity component in the y direction, respectively. The particle is continuously accelerated until the condition breaks.

In the non-relativistic case, γ_p ≈ 1, for the particle is trapped in the wave (v_z=v_p), v_y=(c²-v_p²)^{1/2} holds, and the trapping condition becomes as:

$$E_m > \gamma_p (c^2 - v_p^2)^{1/2} B_0 \approx \gamma_p (c^2 - v_p^2)^{1/2} B_0 = cB_0 \quad (2)$$

This formula represents the trapping condition for the nonrelativistic case and is referred later in Sec. IV. to explain the experimental results.

Energy gain in steady state for a unit length is the same as that originally obtained on the surfatron,

$$\frac{d\gamma}{dy} = \gamma_p \frac{\gamma_p c v_p}{c^2} \quad (3)$$

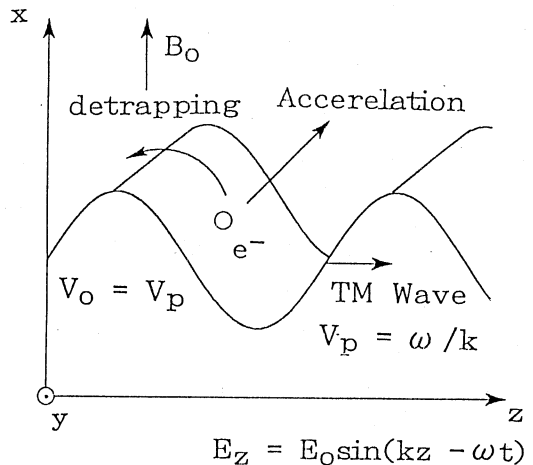
$$\frac{d\gamma}{dz} = \gamma_p \frac{\omega_c^2 z}{c^2} \left(1 + \frac{\omega_c^2 z^2}{c^2} \right)^{1/2} \quad (4)$$

where γ=[1-(v/c)²]^{-1/2} and ω_c is the electron cyclotron frequency. It is seen that dγ/dy is γ_p times as large as dγ/dz, if the two conditions v_p ≈ c and ω_c²z²/c² >> 1 are taken into account, that is, for γ_p > 1 the acceleration rate in the y direction is more efficient than in the z direction. Therefore, L_y/L_z=(γ_p²-1)^{-1/2} ≈ 1/γ_p (γ_p >> 1), where L_y and L_z are the length in the y and z directions respectively required to yield the same amount of energy after acceleration.

Experiments

Figure 2 is a schematic diagram showing an electron beam gun, a slow wave structure and an energy analyzer. The injected electron is initially accelerated by a high voltage power supply, with maximum energy and current of 100 keV and 1 mA, respectively. A hair-pin type cathode is made of a tungsten filament which is originally made for an electron microscope.

The accelerated electrons through the accelerator are detected by an electron energy analyzer which consists of a pair of permanent magnets yielding a



Schematic diagram of the v_pxB acceleration scheme.

uniform magnetic field of 200 G. This instrument is calibrated with the above-mentioned electron source. The calibration is carried out by changing the acceleration voltages without RF power before and after the main experiments. The electrons are detected by an MCP (micro channel plate) across which a voltage of -1.7 kV is applied. The MCP is scanned in the analyzer and the position at which the signal detected from the MCP corresponds to the energy and the signal intensities to the electron fluxes. Therefore this instrument outputs independent two signals. The amplified electron signal is led to the box-car averager. After the integration by it, the output signal is connected to the y-axis of the x-y recorder and the signal for the position is to the x-axis. The resultant electron energy spectrum is drawn on the x-y recorder chart.

The pulsed electromagnetic wave is generated by a magnetron which is triggered by the external timer with a typical pulse width of $5 \mu\text{s}$ in repetition at 10 Hz. We used two different power sources, one has a maximum power of 2.5 kW and the other has 10 kW, the emitted frequencies of them were measured by comparing with the standard oscillator to give 2.465 GHz and 2.459 GHz, respectively. Although both of the original specifications are 2.45 GHz, the frequencies were upper-shifted due to too much of the applied cathode voltages so as to obtain higher output power. The generated microwave is converted into TM wave through the slow wave structure, and is absorbed by a non-reflection dummy load.

The static, vertical magnetic field for a $v_{\text{p}} \times B$ acceleration is generated by a pair of saddle shaped external coils with the uniform length 32 cm (less than 3% uniformity; 40 cm for 5%) in the z direction and 5 cm (less than 3%) in the y direction. A maximum field strength of 10 G is measured at the center of the accelerator. This value should be strong enough to demonstrate the $v_{\text{p}} \times B$ principle in the experimental parameters.

A schematic view of the slow wave structure of the TM mode is shown in Fig. 3. This structure consists of parallel fin electrodes with 48 cm long in the wave propagation direction. Its propagation mode of the microwave is designed to be $2\pi/3$ mode and the phase velocity is $0.464c$ (corresponding energy of 66 keV) at the RF frequency of 2.45 GHz. The cross section of the structure is rectangular. In general the circular type acceleration cavity is popularly used for the linear accelerator to generate the maximum longitudinal electric field at the center of the cavity. In the $v_{\text{p}} \times B$ scheme, however, the electron orbit is parabolically bent by the external magnetic field, in other words, the electron is accelerated in two dimensional. Although the maximum electric field strength is weaker in the present case, we can choose the structure with no obstacles in the y direction. This

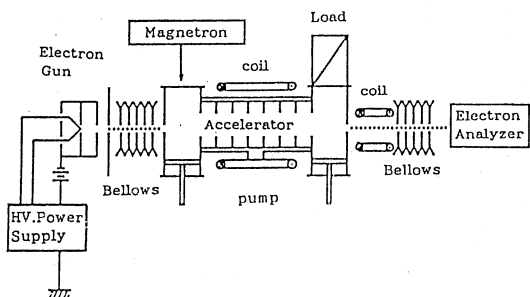


Figure 2.

Experimental apparatus for a proof of the principle of the electron linear accelerator based on the $v_{\text{p}} \times B$ acceleration scheme.

is convenient to demonstrate the $v_{\text{p}} \times B$ acceleration principal. When it works in a relativistic regime, the particle orbit is strictly linear and the circular type slow wave structure could be employed so as to obtain a strongest field.

An example of experimental results with rf power of 2.5 kW is shown in Fig. 4. The horizontal and vertical axes indicate the incident electron energy E_0 and the energy increment $\Delta \epsilon$, respectively. Symbols, \square , \triangle and \circ stand, respectively, for the value of the external magnetic field of 0, 2 and 3 Gauss. When $B_0 = 0$ G, the accelerator operates as the conventional linac. Therefore one can easily compare the $v_{\text{p}} \times B$ accelerator with the conventional one in a same machine. The slow wave structure strongly resonates with the microwave around $E_0 = 48$ and 57 keV. Data show that the energy increment of the $v_{\text{p}} \times B$ scheme is larger than that of the conventional one at every incident electron energy. When the incident beam energy is 48 keV, for example, the observed electron energy is 56 keV ($\Delta \epsilon = 8$ keV) with a static magnetic field of 3 G, while in the conventional accelerator the energy reaches 52.0 keV corresponding $\Delta \epsilon = 4.0$ keV. The expected energy increment is calculated from Eqs.(3) and (4) for the case of $B_0 = 3$ G at $E_0 = 48$ and 56 keV. The results are shown by the solid circles in Fig. 4. The disagreement between the experiment and the calculated value is explained as follow; The Eqs.(3) and (4) are valid only for the steady state of the acceleration only. In the experiment, however, the electrons are not in the steady state but oscillate around the equilibrium point in the phase space because the acceleration time is not sufficient to reach the steady state. Sufficient acceleration condition ($\omega t \gg 1$; in the present machine $t > 20$ nsec is required) is assumed in Eqs. (3) and (4).

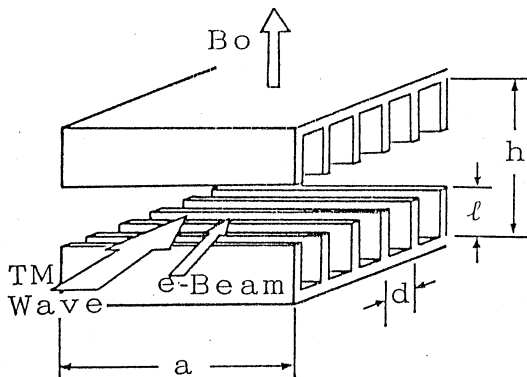


Figure 3.

A schematic structure of the slow wave structure.

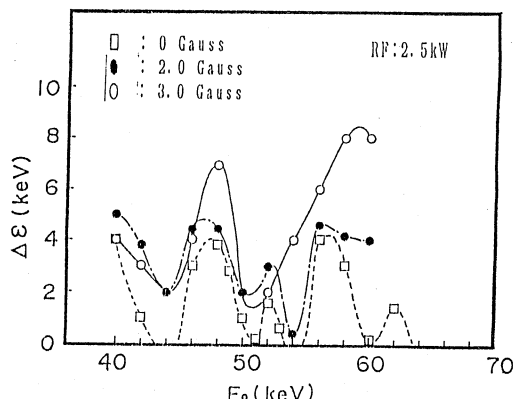


Figure 4.

Energy increment $\Delta \epsilon$ as a function of the incident electron energy E_0 .

Figure 5 shows the energy increment as a function of the static magnetic field intensity. Up to 2 G, the energy increment $\Delta \varepsilon$ is proportional to B^2 , i.e., $\Delta \varepsilon - \Delta \varepsilon(B_0 = 0 \text{ G}) \propto B^2$, while over 2 G, $\Delta \varepsilon$ decreases sharply. This dependence can easily be explained by the Lorentz force acceleration in the y direction. After the value of B_0 exceeds 2 G, the electron cannot be trapped by the wave potential anymore. These results mean that the trapping condition is no longer maintained. The underlying physics producing a critical magnetic field $B_c = 2 \text{ G}$ is explained in the following section.

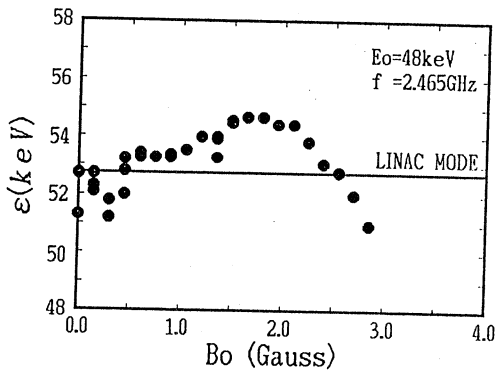


Figure 5.

Energy increment $\Delta \varepsilon$ as a function of the static magnetic field.

Discussion

As seen in Eq. (2), the trapping condition is $v_E = E_m/B_0 > c$, i.e., the electrons are continuously accelerated until the trapping condition breaks down. The experimental parameters are listed in Table 1. The electric field E_m was obtained from the relation between the energy increment of the conventional linac mode and the length of the accelerator cavity. B_{exp} indicates the magnetic field under which the maximum acceleration energy is attained. Here v_E is normalized by the speed of light c . At every incident energy, v_E is smaller than c , that is, the trapping condition was not satisfied in the experiments. However, above results cannot give the information of the time when electrons detrap from the wave potential. The detraping time t_c can be determined by the equation,¹²⁾

$$\omega t_c = \frac{\delta}{(1-\delta^2)^{0.5}} - \cos^{-1} \delta + kz(0) - \frac{kv_x(0)}{\omega} \quad (5)$$

where $\delta = \omega_c^2 / \omega_b^2 \ll 1$, $\omega_c = qB_0/m$ and $\omega_b^2 = qE_m k/m$. To explain the experimental data, assuming $z = 0$, $v_x = 0$ at $t = 0$, one can obtain using $\delta \ll 1$, Eq.(5) is rewritten as

$$\omega t_c = 1/\delta. \quad (6)$$

The time τ is a time duration of the electron traveling with a constant velocity corresponding to the incident energy. The differences τ and t_c vary from

Table 1.

Experimental parameters of the electron trapping.

E_0 (keV)	E_m (kV/m)	B_{exp} (G)	v_E (xc)	t_c (ns)	τ (ns)	P (kW)
48	9.6	1.8	0.18	5.6	4.0	2.5
62	16.6	2.6	0.21	4.7	3.5	10
66	20.0	2.6	0.26	5.6	3.5	10

1.1 to 2.2 nsec. Although the experimental data and the calculated results are slightly different, it is shown that these are in fairly good agreement after taking into account of the following conditions; The incident electron is injected obliquely to the z axis, so that the value of τ is greater than that of the tabulated. When the present machine is used as a conventional linear accelerator without a static magnetic field, the electron beam is adjusted to traverse the region with maximum field strength in the slow wave structure. In other words, the maximum particle energy could be reached in the conventional mode. In the case of v_{pXB} accelerator, however, the orbit of the electron beam bends slightly, because of the slow beam velocity, and the electron cannot travel in the area with the maximum field strength. Therefore the existence of the critical magnetic field (1.7 G at 48 keV, 2.7 G at 62 and 66 keV) can be interpreted by the present theory.

Conclusion

A new electron linear accelerator based on the v_{pXB} acceleration scheme has been demonstrated to work successfully in a vacuum system. The experimental results show that proposed scheme accelerates the electron more effectively than the conventional linear accelerator. The measured data are in good agreement with the theoretical results containing weak relativistic effects.

Acknowledgment

The authors are indebted to Professor R. Sugihara and Dr. S.Takeuchi for discussions. A part of the present work has been supported by the Grant-in-Aid for Scientific Research from the Ministry of Education, Science and Culture, Japan.

References

- 1) T. Tajima and J. M. Dawson, Phys. Rev. Lett. 43, 267-270 (1979).
- 2) P.Chen, J. M. Dawson R. W. Huff and T. Katsouleas, Phys. Rev. Lett. 54, 693-696 (1985).
- 3) R. Sugihara and Y. Mizuno, J. Phys. Soc. Jpn. 47, 1290-1295 (1979).
- 4) Y. Nishida, M. Yoshizumi and R. Sugihara, in Proceedings of the Thirteenth Annual Anomalous Absorption Conference, Banff, Alberta, Canada, 5-10 June 1983, (unpublished) p.F7; Phys. Lett. 105A, 300-302 (1984); Y. Nishida, M. Yosizumi and R. Sugihara, Phys. Fulids 28, 1574-1576 (1985).
- 5) C. Joshi and T. Katsouleas, in Laser Acceleration of Particles, edited by C. Joshi and T. Katsouleas, AIP Conf. Proc. No. 130 (AIP, New York,1985).
- 6) T. Katsouleas and J. M. Dawson Phys. Rev. Lett. 51, 392-395 (1983).
- 7) Y. Nishida, N. Yugami, H. Onihashi, T. Taura and K. Otsuka, Phys. Rev. Lett. 66, 1854-1857 (1991), and references therein.
- 8) A.Loeb and L. Friedland, Phys. Rev. A 33, 1828-1835 (1986).
- 9) S. Takeuchi, K. Sakai, M. Matsumoto and R. Sugihara, Phys. Lett. A122, 257 (1987).
- 10) Y. Nishida, in Laser Interaction and Related Plasma Phenomena, edited by H. Hora and G. Miley (Plenum, New York, 1986), Vol. 7, pp. 811-825.
- 11) Y. Nishida, in Proceedings of the Nineteenth International Conference on Phenomena in Ionized Gases, Invited Papers, (July 10-14 1989, Belgrades, Yugoslavia) edited by Vida J. Zigman, pp. 186-194; A Variety of Plasma, Proceedings of the 1989 International Conference on Plasma Physics, edited by A. Sen and P. K. Kaw. Indian Academy of Sciences, pp. 39-55.
- 12) Y. Terashima, J. Phys. Soc. of Jap. 30, 2210-2217, (1991)